



DESCRIPTION OF THE PROJECT RESULTS

1. Aerodynamic concept of the CLC-System.

The Closed-Loop Control System for fluidic active flow control was proposed to improve the wing high lift devices performance (especially to delay the flow separation and increase the lift coefficient). The CLC-system has been tested experimentally on a two dimensional airfoil model equipped with movable flap. Wind tunnel tests were preceded by numerical calculation. Numerical simulations were conducted to develop a general concept of aerodynamic object being a basis for the proposed CLC-system for fluidic active flow control. Several different concepts were considered. Finally, the concept described below has been chosen.

The general idea of the realized CLC-system is shown in Fig.1. As a subject of the research, the high-lift wing segment, built based on airfoil NACA0012 and equipped with the 30% slotted flap, has been used. The flap is deflected usually in takeoff and landing flight conditions to increase a lift force of the wing.

Start Date of ESTERA: 1st December 2011 Duration: 15 Months

ESTERA is coordinated by: IoA – Institute of Aviation

This document has been produced by the ESTERA consortium under FP7 of the EU. Copyright and all other rights are reserved by the partners in the ESTERA consortium.

The release of this report is RESTRICTED

Any disclosure or distribution outside of ESTERA
and the European Commission is prohibited and may be unlawful.

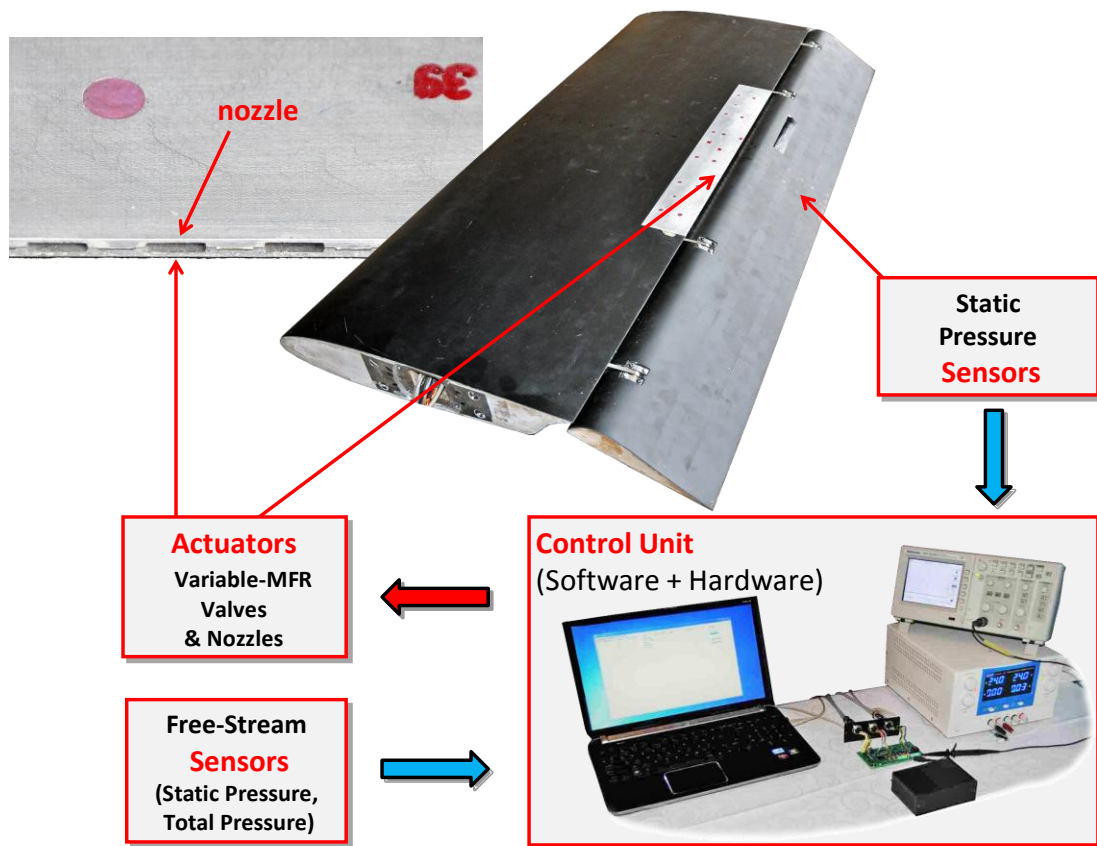


Figure 1: Aerodynamic concept of the CLC-System

2. Description of the CLC-System Prototype

2.1. Introduction to the CLC-System Prototype description

A typical Closed Loop Control system is a control system which uses sensor measurement F of the system output $y(t)$ to compare it to the reference value $r(t)$. The controller C then takes the error e (difference between the reference and the output) to change the inputs u to the system under control P . This is shown in Figure 2 and such system is called a single-input-single-output (SISO) control system; *MIMO* (i.e. Multi-Input-Multi-Output) systems, with more than one input/output, are common. In such cases variables are represented through vectors instead of simple scalar values. For some distributed parameter systems the vectors may be infinite-dimensional (typically functions). Every control system must guarantee first the stability of the closed-loop behavior.

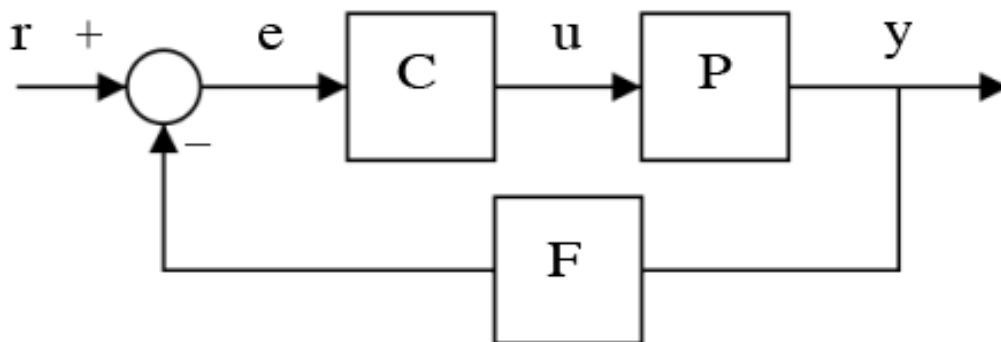


Figure 2: Closed-Loop Control system

Controllability and observability are main issues in the analysis of a system before deciding the best control strategy to be applied, or whether it is even possible to control or stabilize the system. Controllability is related to the possibility of forcing the system into a particular state by using an appropriate control signal. If a state is not controllable, then no signal will ever be able to control the state. If a state is not controllable, but its dynamics are stable, then the state is termed stabilizable. Observability instead is related to the possibility of "observing", through output measurements, the state of a system. If a state is not observable, the controller will never be able to determine the behaviour of an unobservable state and hence cannot use it to stabilize the system. However, similar to the stabilizability condition above, if a state cannot be observed it might still be detectable.

Several different control strategies have been devised in the past years. These vary from extremely general ones (PID controller), to others devoted to very particular classes of systems (especially robotics or aircraft cruise control).

A control problem can have several specifications. Stability, of course, is always present: the controller must ensure that the closed-loop system is stable, regardless of the open-loop stability. A poor choice of controller can even worsen the stability of the open-loop system, which must normally be avoided.

Another typical specification is the rejection of a step disturbance; including an integrator in the open-loop chain (i.e. directly before the system under control) easily achieves this. Other classes of disturbances need different types of sub-systems to be included.

Other "classical" control theory specifications regard the time-response of the closed-loop system: these include the rise time (the time needed by the control system to reach the desired value after a perturbation), peak overshoot (the highest value reached by the response before reaching the desired value) and others (settling time, quarter-decay). Frequency domain specifications are usually related to robustness.

Modern performance assessments use some variation of integrated tracking error (IAE, ISA, CQI).

For linear systems, this can be obtained by directly placing the poles. Non-linear control systems use specific theories (normally based on Aleksandr Lyapunov's Theory) to ensure stability without regard to the inner dynamics of the system. The possibility to fulfill different specifications varies from the model considered and the control strategy chosen.

The PID controller is probably the most-used feedback control design. PID is an acronym for Proportional-Integral-Derivative, referring to the three terms operating on the error signal to produce a control signal. If $u(t)$ is the control signal sent to the system, $y(t)$ is the measured output and $r(t)$ is the desired output, and tracking error $e(t) = r(t) - y(t)$, a PID controller has the general form

$$u(t) = K_P e(t) + K_I \int e(t) dt + K_D \frac{d}{dt} e(t).$$

The desired closed loop dynamics is obtained by adjusting the three parameters K_P , K_I and K_D , often iteratively by "tuning" and without specific knowledge of a plant model. Stability can often be ensured using only the proportional term. The integral term permits the rejection of a step disturbance (often a striking specification in process control). The derivative term is used to provide damping or shaping of the response. PID controllers are the most well established class of control systems: however, they cannot be used in several more complicated cases, especially if MIMO systems are considered.

2.2. CLC-System hardware

This section contains description of all major parts of the designed hardware platform. All major parts of the controller are presented in Figure 3 and cover:

- 4 inputs for pressure sensors (analog or digital interface)
- 2 outputs for electromagnetic valves
 - 2 modes of operation: ON/OFF or PWM
 - Feedback signal - control output current
- CAN interface
- USB 2.0 diagnostic interface
- Single supply operation (15 – 36VDC), typical supply voltage 28VDC

The block diagram of the CLC-System prototype architecture is similar to the mock-up concept that was verified against experience gained during mock-up testing and acquired wind tunnel results.

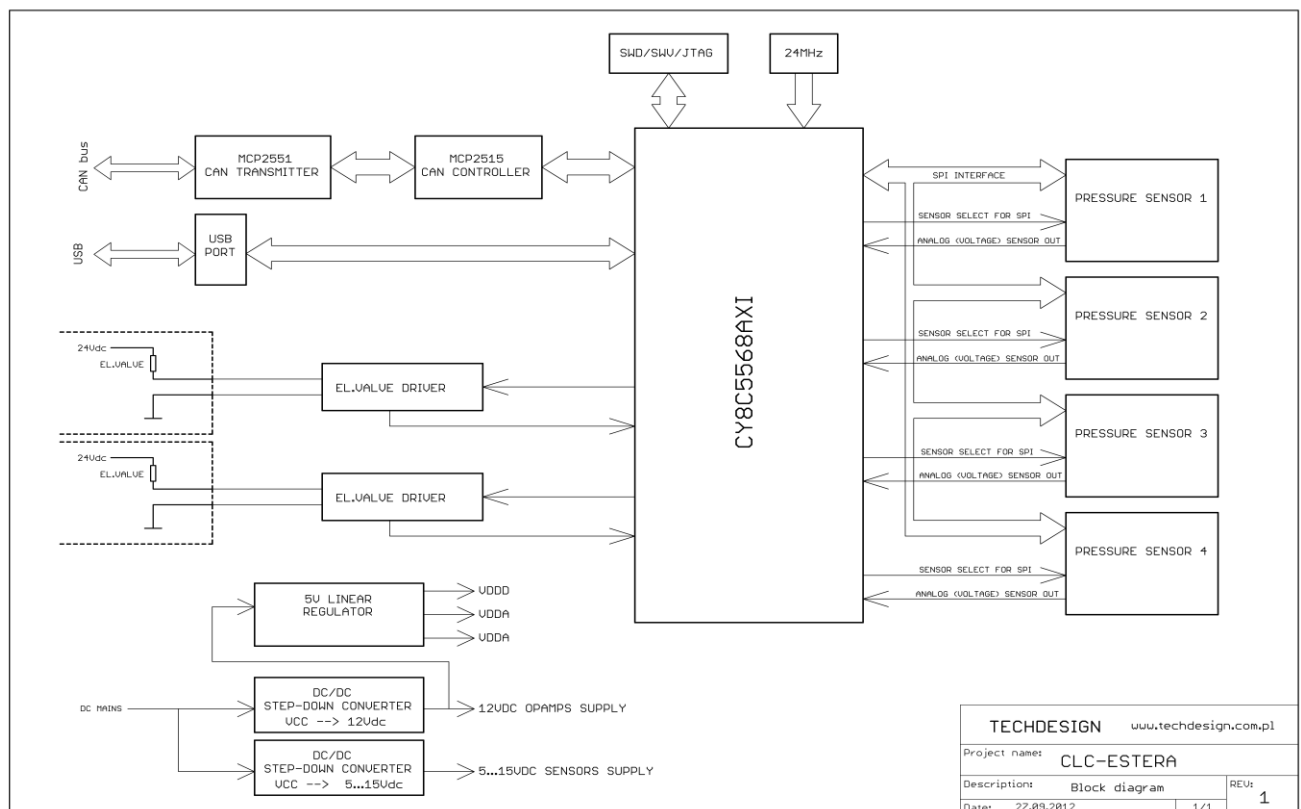


Figure 3: CLC-System Hardware - block diagram

Processor

The design is based on CY8C55xx series controller. It is a family of PSoC (Programmable embedded System-on-Chip) from Cypress. PSoC architecture features:

- Integrated high-precision 20-bit resolution analog subsystem,
- Programmable PLD-based logic subsystem,
- 32-bit ARM® Cortex™-M3 CPU up to 67 MHz,
- Power and clock management subsystems,
- Integrated debug and tracing mechanisms.

PSoC is clocked using 24MHz crystal resonator. Apart from USB link circuitry, an on board programming and debugging connector has been installed which employs MiniProg3 programmer from Cypress.

Communication interfaces

The module has been equipped with two interfaces: CAN (Controller Area Network) for communication between modules and host computer and USB (Universal Serial Bus) link which enables data transmission to host computer (dedicated for service and diagnostic).

Pressure sensors inputs

The circuit is designed for two types of sensors: analog voltage and digital (SPI interface) output. For analog sensors voltage output signal is fed to the input of the ADC through the operational amplifier as a buffer and resistive divider. Transil and Zener diode protects the ADC against voltage surges, Figure 4.

Digital sensors use SPI interface (common lines MISO (Master Input Slave Output) and SCLK (Serial Clock)). Each sensor has its own signal CS (Chip Select), Figure 5.



Figure 4: Pressure sensor input (analog version) – block diagram

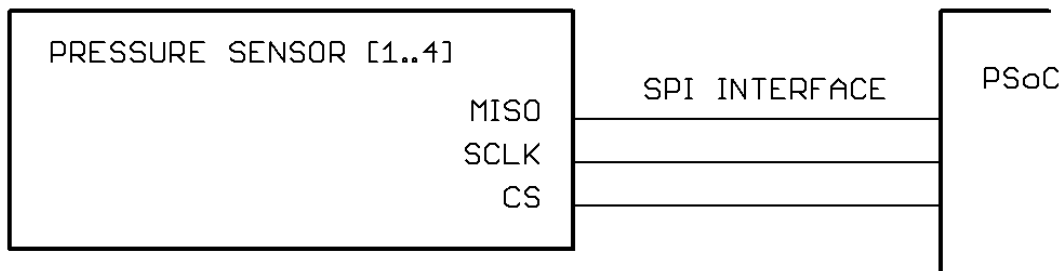


Figure 5: Pressure sensor input (digital version) – block diagram

There are three sources of power the sensors, Figure 6:

1. 5VDC from VDDA – dedicated for digital sensors
2. High precision 3.3VDC or 5VDC from reference voltage source
3. VCCADJ from DC-DC converter - when you need a voltage greater than 5VDC.

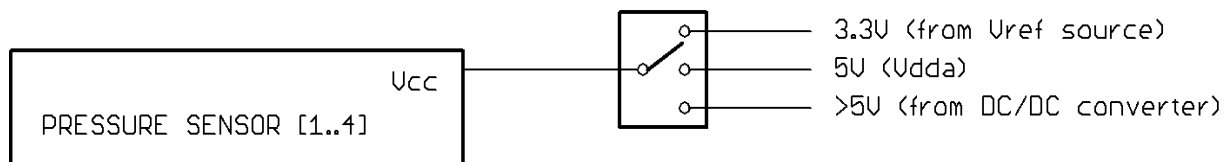


Figure 6: Pressure sensors supply – block diagram

Electromagnetic valves outputs

The module has two solenoid outputs. There are two modes of operation: control the ON/OFF or PWM signal. For this reason, the actuators used are fast MOSFET transistors. Transistors used work well with TTL control signal and require no additional signal forming circuit. A small resistance $R_{ds(on)}$ and high speed switching allow to work this transistors without additional heat sink, Figure 7.

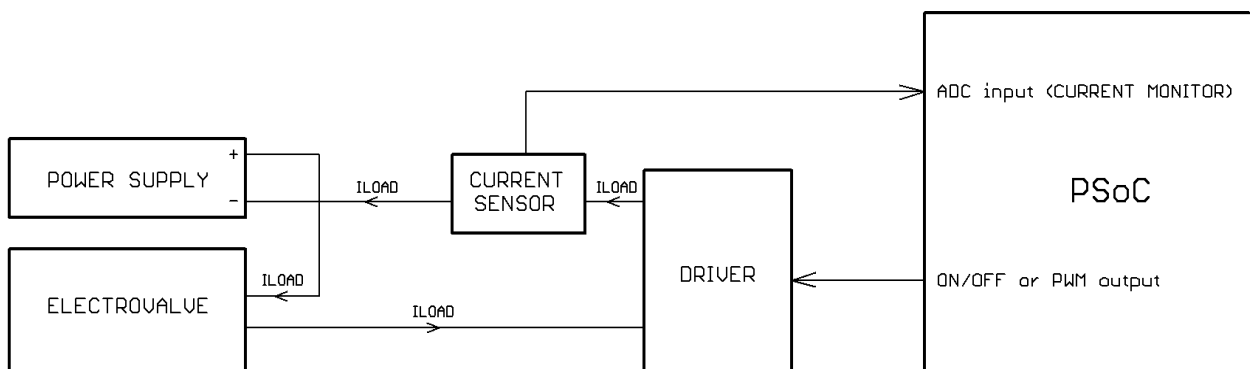


Figure 7: Electromagnetic valves output – block diagram

Power supplies

The circuit is designed to supply the DC voltage range from 15 to 36VDC. The power supply consists of two DC-DC converters and one linear regulator, Figure 8. Provides supply voltages:

- +12VDC for operational amplifier and for linear regulator
- DC from 5V to 15V for pressure sensors (optional)
- +5V for digital and analog parts, processor and communication circuit.

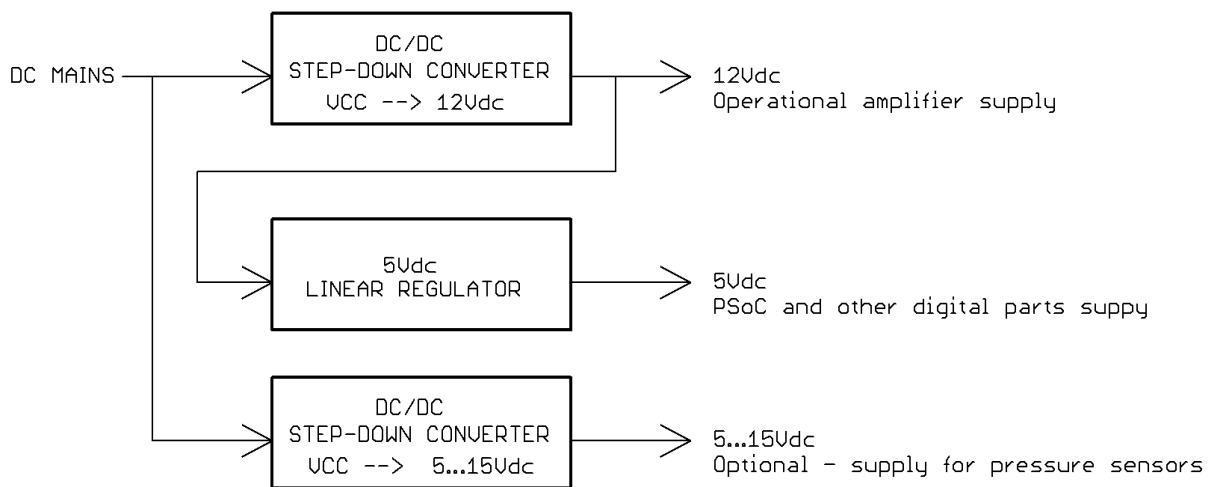


Figure 8: Power supplies – block diagram

2.3. CLC-System Embedded software

CLC-System prototype hardware differs from the mock-up solution significantly and as a result the software designed for the prototype offers much more functionality.

The controller can operate in three main modes:

- Idle,
- Manual control,
- Automatic control.

Idle mode is dedicated to all measurement and control parameters monitoring and logging. It is intended for system diagnostic and maintenance purposes and does not enable actuator control / activation.

Manual control mode is intended for output power stage and actuator circuitry testing and calibration.

Automatic control mode is the most important, normal (AFC algorithm based) operation mode. In this mode the system executes selected control algorithm with its parameters established at the set-up stage. A typical control cycle diagram is presented in Figure 9.

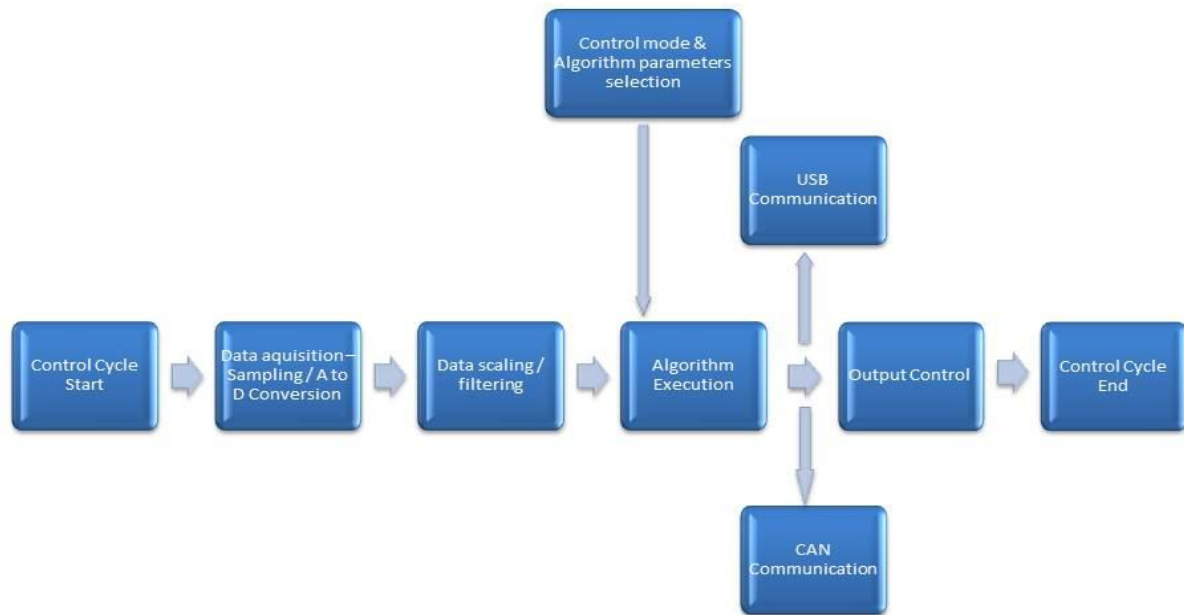


Figure 9: Cycle diagram Control

Cycle time of the control loop has been established to the value which assures all tasks are fully completed during one cycle. On the other hand the cycle time should be constant to collect measured parameters and execute algorithm using the same base time period. Figure 10 shows typical cycle timing.

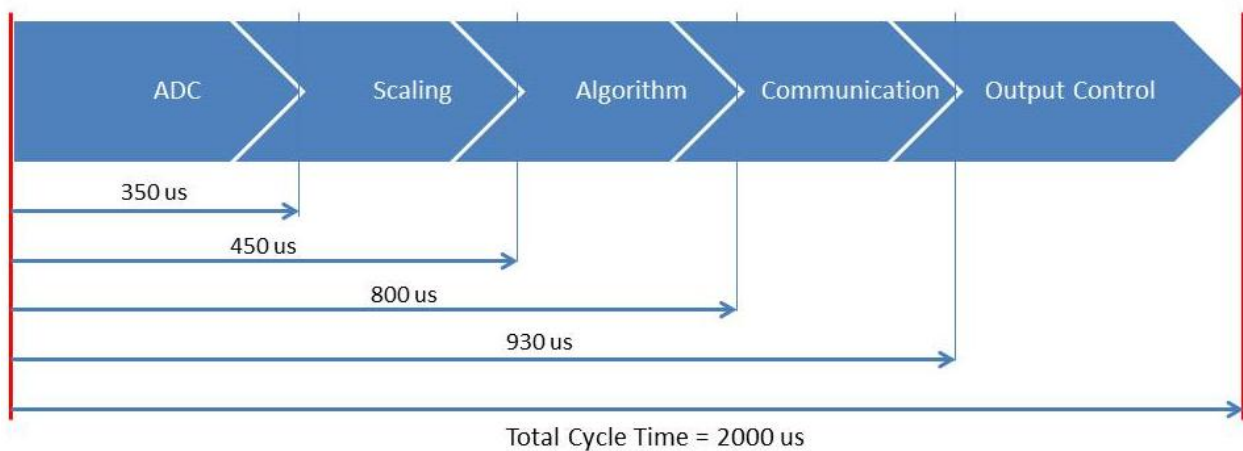


Figure 10: Typical cycle timing

The software is implemented using PSoC 2.2 Creator IDE provided by Cypress Semiconductors, which consists of two parts:

- graphical design editor where MCU peripherals are configured and connected,
- C language programming editor for MCU.

MCU program is divided into four modules, Figure 11:

- ADC-Manager module – responsible for data acquisition and computing converted ADC values to voltage and pressure. Analog to Digital conversion is triggered by periodic timer interrupt,
- Algorithm module – contains group of algorithms that may be used for output control. There are three output control types:
 - regular 8bit PWM with fixed period set to 768ms (resolution ~3ms) – pulse width depends on value computed by the module,
 - duty cycle set to 50% with configurable period (2-20ms) and output counter which kills the PWM block when configured counting value is reached
 - bi-state output – sets output to ‘high’ when computed output value is larger than 0, otherwise sets output to ‘low’ state,
- USB module – connects the controller with PC (ServiceApp), sends voltage/pressure values and computed results to PC and receives and sets parameters defined in ServiceApp,
- CAN module – communicates with MCP2515 CAN controller chip via SPI interface which is capable of transmitting and receiving data over CAN interface. Functionality of this module is quite similar to the USB module. The following values are sent over CAN interface: pressure, output value, Cp.

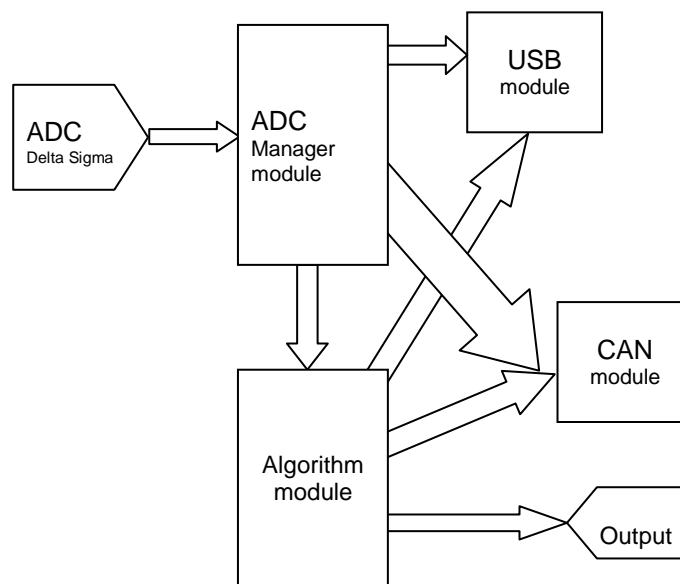


Figure 11: Embedded software modules and their interactions

ServiceApp

Service application is an interface that gives an opportunity to configure, gather and present current data received from Estera controller. The program is written in Python 2.7 language with two additional packages: xwPython (cross platform GUI toolkit) and pySerial (serial port encapsulation for Python) consists of two parts which graphically will be presented by tabs. Configuration is the first one that contains several elements gives opportunity to set firmware parameters mentioned in previous chapter. The tab provides two actions read and write which may be triggered using corresponding buttons.

The second tab is responsible for data logging. One may choose folder and file name where all received data is stored using .csv format (data values separated by semicolon). The data logging process may be started and stopped by the Start/Stop button. Moreover, all recently received values are presented in the window providing easy data monitoring.

USB2CAN

USB2CAN firmware may be used to program dedicated controller prepared for this purposes and regular Estera controller as well. Main and most important part of this program is to transcode data received from CAN interface (MCP2515 controller chip) and send it to PC over USB.

This program is written for testing purposes.

USB2CANApp

Usb2CanApp is a standalone application written in C# using MS Visual C# 2010 Express IDE and MS .Net Framework 3.0. Prepared for testing purposes the program is used to configure and present all data sent by ESTERA controller via CAN interface. This application displays data from up to four ESTERA controllers. Communication with USB2CAN controller is implemented based on drivers and Cypress Suite USB 3.4.7 framework provided by Cypress Semiconductors.

3. Wind tunnel tests of the CLC-System Prototype

3.1. Experimental setup and instrumentation

The tests were performed in the low speed wind tunnel T-1 (with 1.5 m diameter test section) in the Institute of Aviation, (IoA) Warsaw for Mach numbers $M = 0.1$, 0.075 and 0.05 . The NACA 0012 airfoil segment model of 0.5 m chord, 1 m span and 30% flap (without optimization of the gap between flap and airfoil main body) was used. The model was mounted vertically in the test section between two stationary endplates, Fig.12. The airfoil aerodynamic characteristics were determined by measuring pressure distribution on the model surface. Approximately one hundred measurement orifices of 0.5 mm diameter were distributed on the upper and lower surfaces of the airfoil along its chord (on the flap in four cross sections), Fig.13. Based on the obtained pressure distribution the value of aerodynamic characteristics (lift and moment coefficients) were determined. To calculate the total drag coefficient of the airfoil wake rake measurements were taken. All the pressures (from airfoil and rake) were measured by

pressure system “INITIUM” which consists of the three pressure electronic scanners ESP-32HD.



Figure 12: The NACA 0012 airfoil model with movable flap in the wind tunnel test section

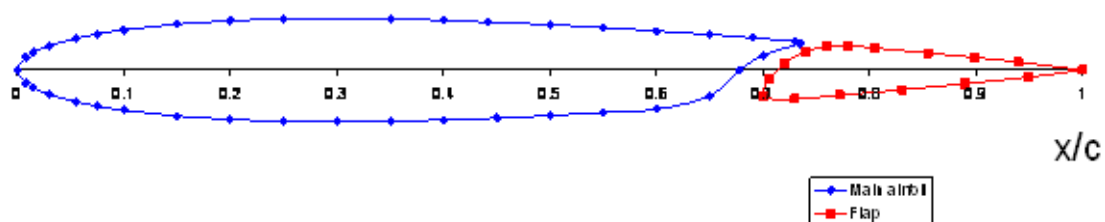


Figure 13: Points of pressure measurement

The main airfoil section was equipped with the row of the 12 triple nozzles situated in its trailing edge (Fig.14). The nozzles' outlet had a rectangular geometric shape with rounded corners (5.6 mm x 1 mm). They were arranged in a such way, that blowing was directed straight into the boundary layer flow on the flap nose. Additional blowing increased the energy in the boundary layer making it more stable and resistant to separation.

The flow through the nozzles was controlled by set of the twelve double position electromagnetic valves (MHE4-MS1H type with controlled operating frequency) mounted inside the model.

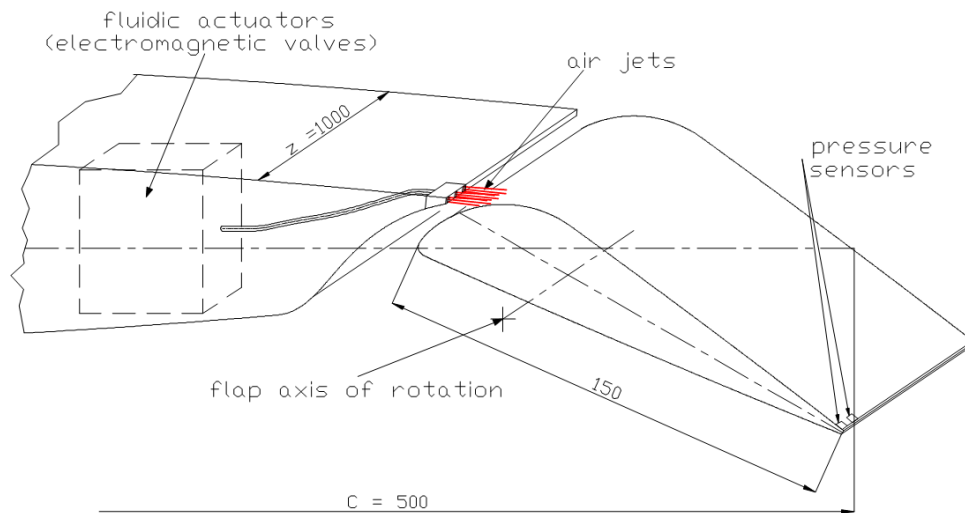


Figure 14: Blowing on the airfoil flap

The coefficient of the pressure measured in the point close to flap trailing edge (as the average of 20 samples) was a parameter defining the state of the flow on the upper flap surface (for the separated flow the pressure value was negative while for attached flow was positive or close to zero). This parameter was analyzed by control system which opened or closed the valves, Fig.1.

During the tests the total volume flow rate of the blown out air was measured by flow-meter.

The model of the NACA 0012 airfoil in low speed wind tunnel T-1 with air supplying system is presented in Fig. 15.

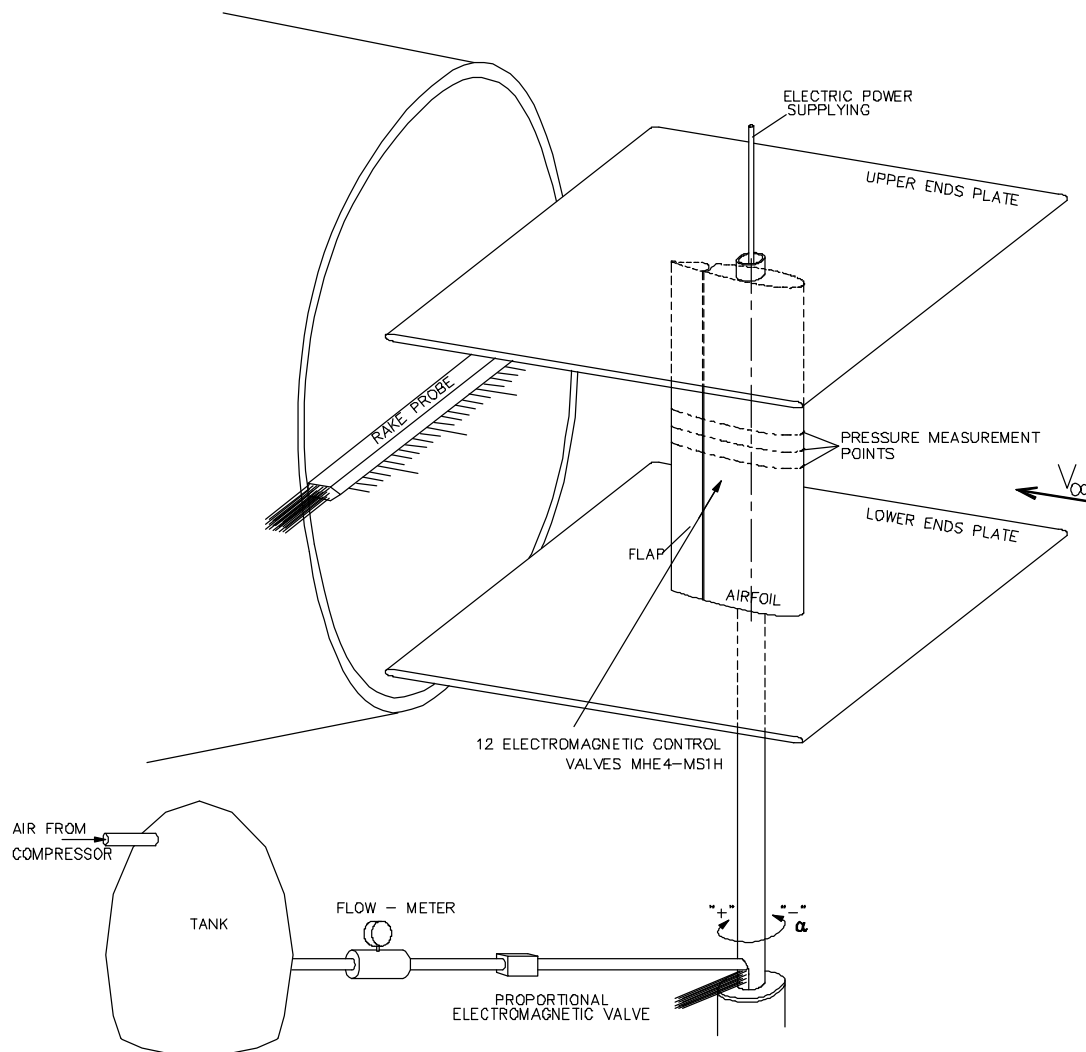


Figure 15: Model of the NACA 0012 airfoil in low speed wind tunnel T-1 with air supplying system.

3.2. Wind tunnel tests program

Wind tunnel tests program of the CLC-System Prototype assumed to investigate the following issues:

- Influence of the value of pressure coefficient (C_{p_c}) used by the CLC-System as a signal for opening or closing the valves on the pressure distribution along the airfoil chord, on the airfoil aerodynamic characteristics and on the air jets volume flow rate.
- Influence of the airfoil NACA 0012 model angle of attack on the pressure distribution along the airfoil chord, on the airfoil aerodynamic characteristics and on the air jets volume flow rate (with using the CLC-System).

- Influence of the undisturbed flow velocity on the pressure distribution on the model surface, on the airfoil aerodynamic characteristics and on the air jets volume flow rate (with using the CLC-System).

All the wind tunnel test were performed with the same sequence of changes in the angle of flap deflection, i.e. initially the flap was deflected from the $\delta = 0^\circ$ up to $\delta = 40^\circ$ with angular speed $\dot{\delta} = 1.4\text{-}1.5$ deg/s, then was kept deflected ($\delta = 40^\circ$) for about 20 seconds and finally restored to the starting position ($\delta = 0^\circ$) with approximately same angular speed. During all these studies CLC-System operated and control the opening or closing the valves. With a fully open electromagnetic valves, the proportional valve (contained in air supplying system, Fig.5) was so positioned that total (from 36 nozzles) air volume flow rate was $\dot{U} \approx 120 \text{ m}^3/\text{h}$ ($V_j \approx 90 \text{ m/s}$).

The detailed program of the wind tunnel tests of the CLC-System Prototype is shown in Table 1. This table shows also average measured volume flow rate (total) during operation of the CLC-System.

Table 1. Wind tunnel test program

Run No	M	V_∞ [m/s]	α [deg]	C_{p_c}	\dot{U}_a [$\pm 5 \text{ m}^3/\text{h}$]
755	0.1	34	10°	0	73
756	0.1	34	10°	-0.1	64
757	0.1	34	10°	-0.2	55
758	0.1	34	10°	-0.3	45
759	0.1	34	10°	-0.4	35
760	0.1	34	20°	0	66
761	0.1	34	20°	-0.1	57
762	0.1	34	20°	-0.2	47
763	0.1	34	20°	-0.3	37.5
764	0.1	34	20°	-0.4	30
765	0.1	34	0°	0	69
766	0.1	34	0°	-0.1	61
767	0.1	34	0°	-0.2	57
768	0.1	34	0°	-0.3	46

769	0.1	34	0°	-0.4	35
770	0.1	34	15°	0	62.5
771	0.1	34	15°	-0.1	55
772	0.1	34	15°	-0.2	46
773	0.1	34	15°	-0.3	37
774	0.1	34	15°	-0.4	29
775	0.05	17	10°	0	63
776	0.05	17	10°	-0.1	55
777	0.05	17	10°	-0.2	46
778	0.05	17	10°	-0.3	38
779	0.05	17	10°	-0.4	30
780	0.075	25.5	10°	0	61.5
781	0.075	25.5	10°	-0.1	53.5
782	0.075	25.5	10°	-0.2	44
783	0.075	25.5	10°	-0.3	35
784	0.075	25.5	10°	-0.4	30

3.3. Wind tunnel test results

The example of wind tunnel test results are presented in Fig. 17. The result of each run includes one plot which presents the influence of the angle of flap deflection on the total airfoil lift coefficient and also 33 small plots, which present the changes in the pressure distribution [$C_p = f(x/c)$] on the upper and lower surface of the flap and rear part of the airfoil main body over time (during the CLC-System operation at $\delta = 40^\circ$). These plots are shown at such order that first presents the moment, when due to CLC-System operation, it begins the growth of the negative pressure on the upper flap surface in the area close it leading edge. They end approximately in the same moment including one full cycle of the CLC-System operation. These small figures do not present the full airfoil pressure distribution along the chord because the pressure changes in the airfoil front part are insignificant, Figure 16.



PROJECT FINAL REPORT

June 2013

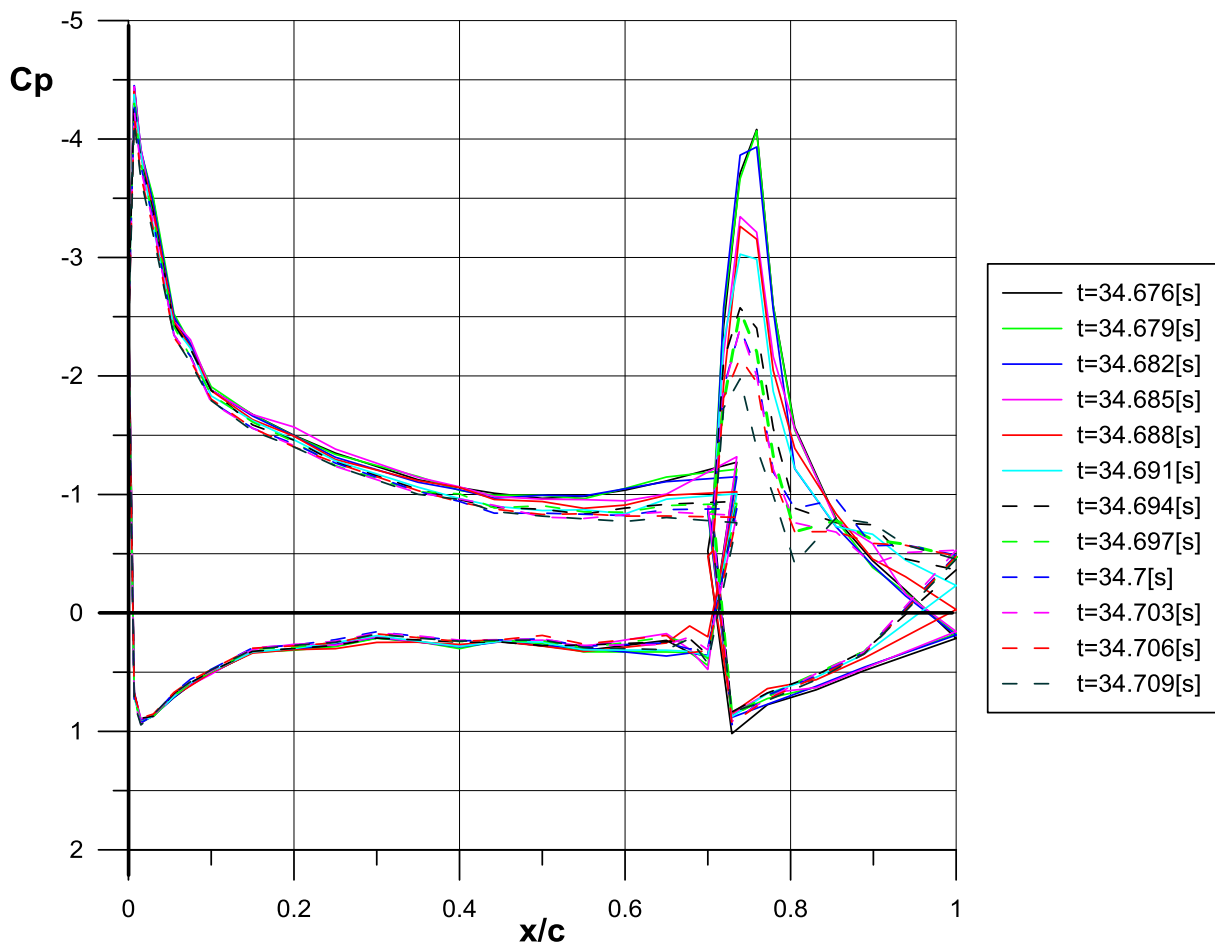
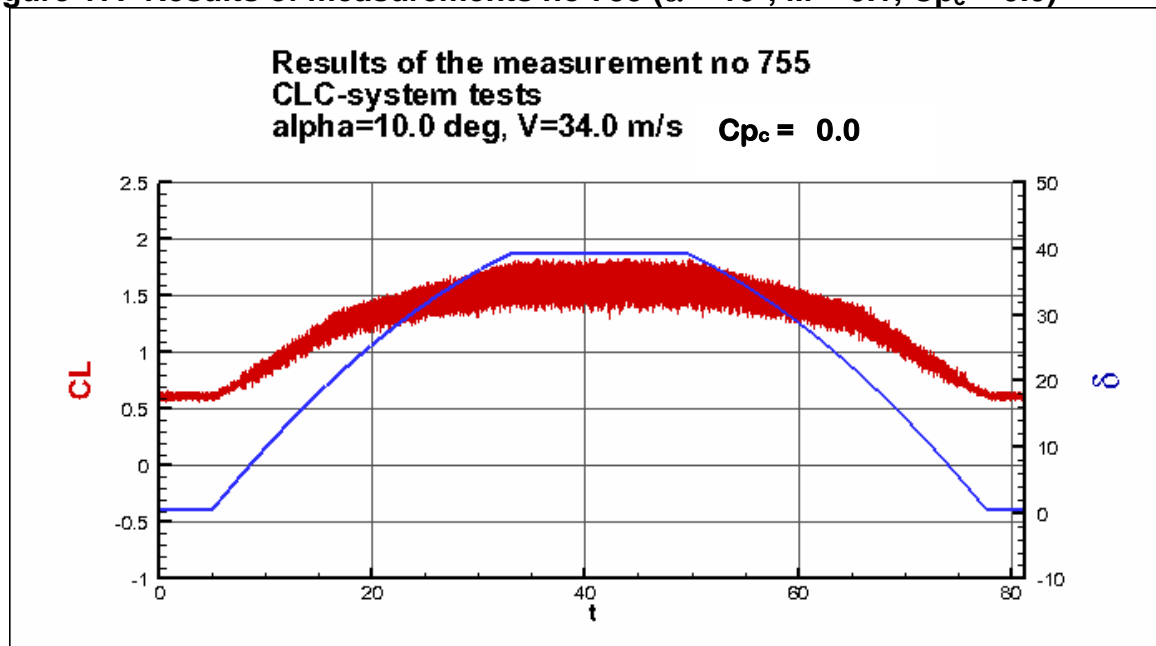
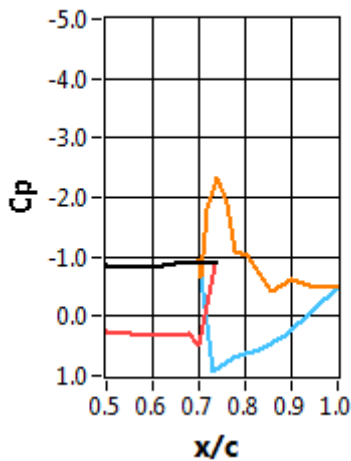


Figure 16: The impact of the CLC-System action on the pressure distribution on the NACA 0012 airfoil surface at the $M = 0.1$, $\alpha = 10^\circ$, $\delta = 40^\circ$ and $C_{p_c} = -0.1$

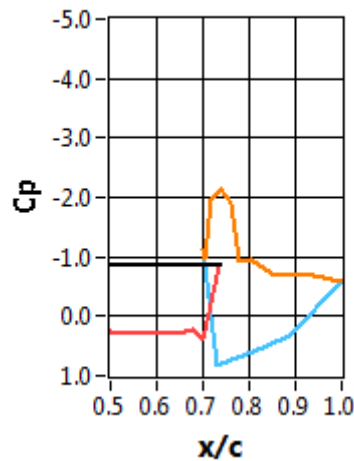
Figure 17: Results of measurements no 755 ($\alpha = 10^\circ$, $M = 0.1$, $C_{p_c} = 0.0$)



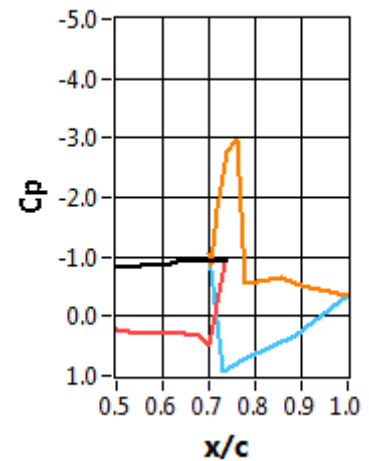
Time=41.389 s, CL=1.487



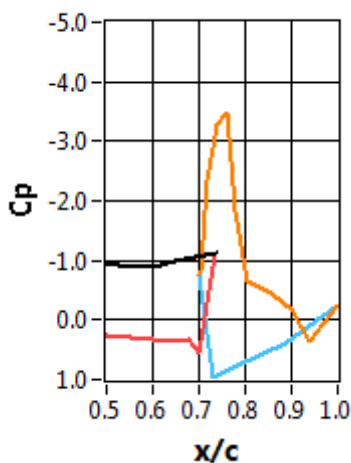
Time=41.391 s, CL=1.483



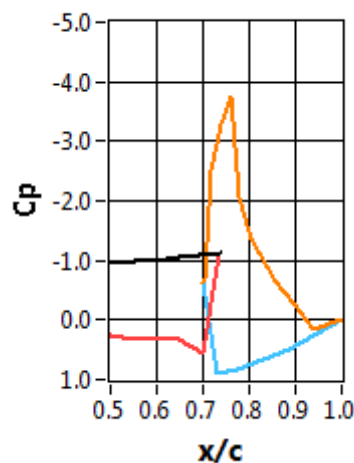
Time=41.394 s, CL=1.487



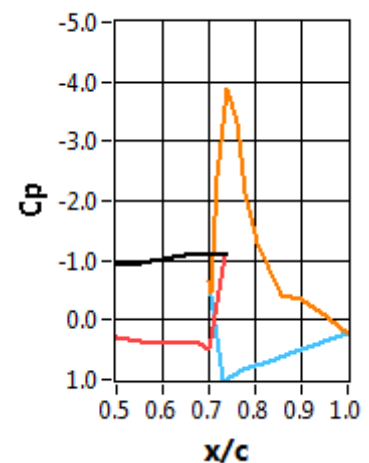
Time=41.397 s, CL=1.551

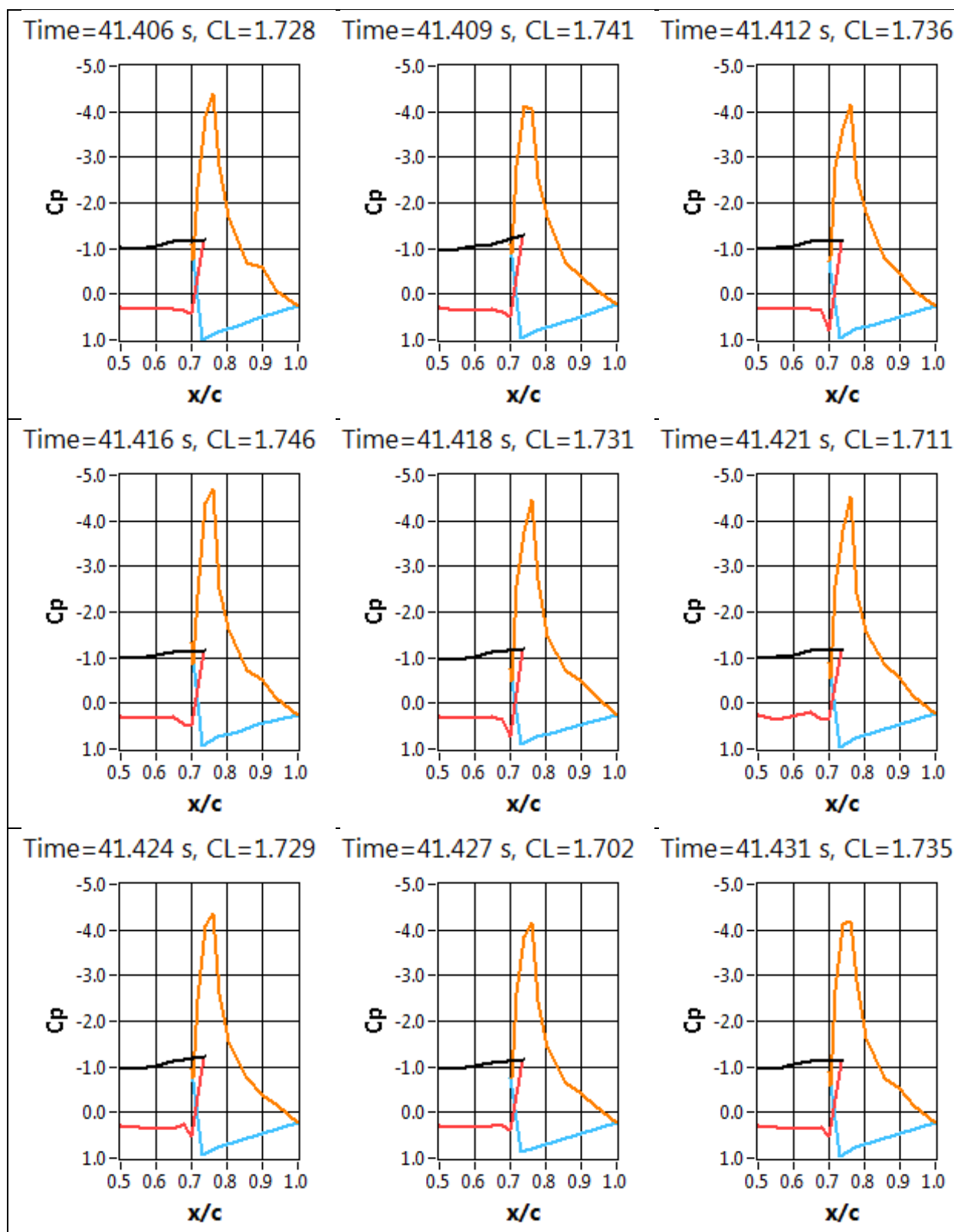


Time=41.400 s, CL=1.632

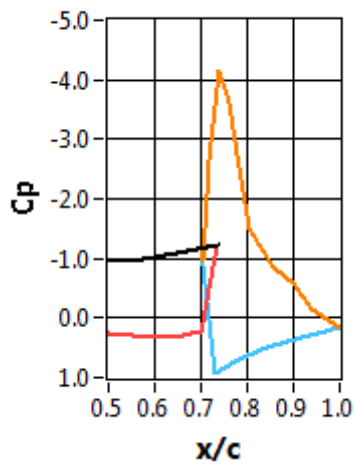


Time=41.403 s, CL=1.662

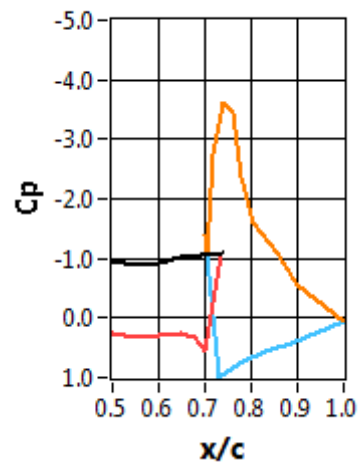




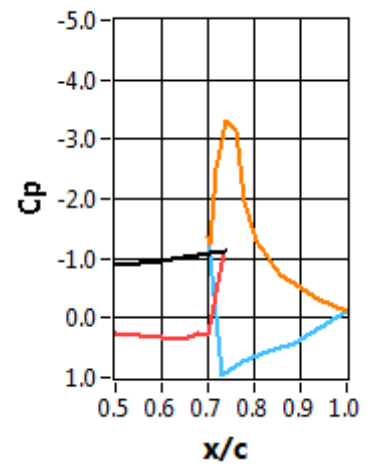
Time=41.434 s, CL=1.701



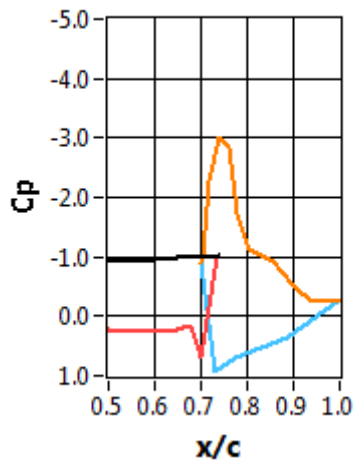
Time=41.437 s, CL=1.691



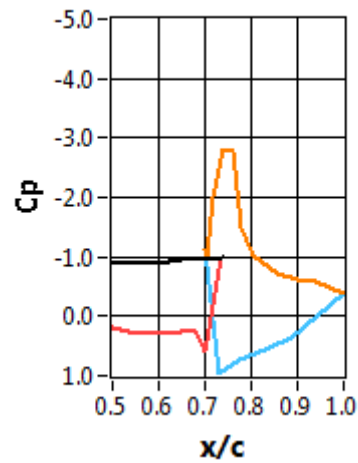
Time=41.440 s, CL=1.632



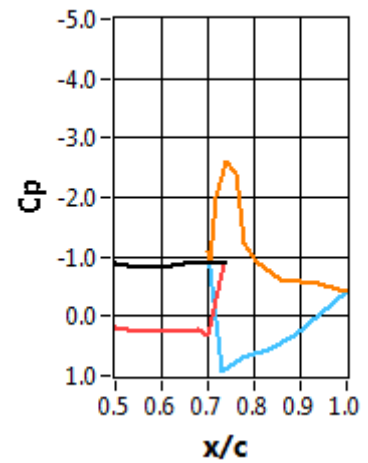
Time=41.443 s, CL=1.585



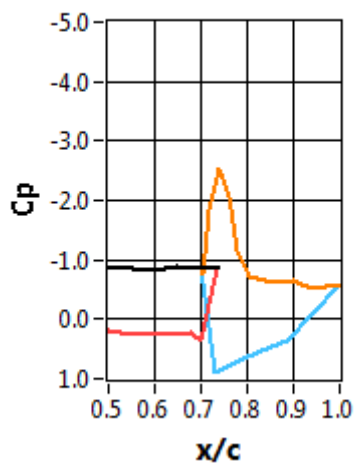
Time=41.447 s, CL=1.556



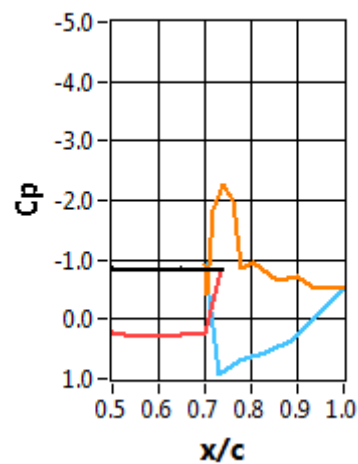
Time=41.449 s, CL=1.496



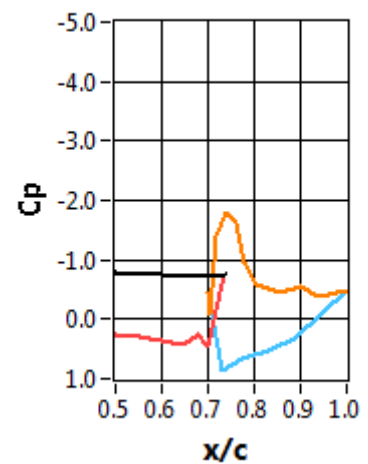
Time=41.452 s, CL=1.461



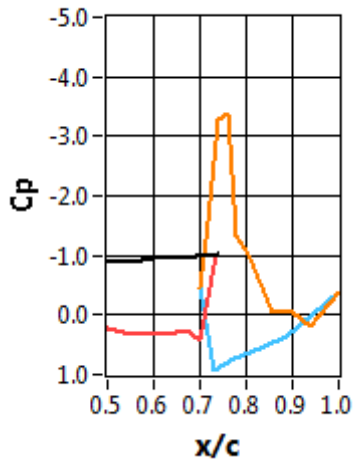
Time=41.455 s, CL=1.447



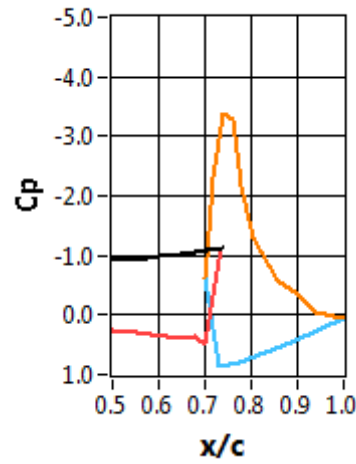
Time=41.458 s, CL=1.376



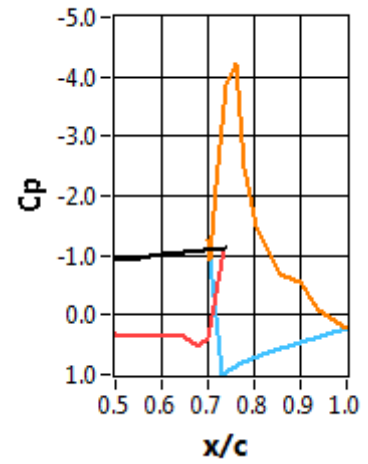
Time=41.461 s, CL=1.487



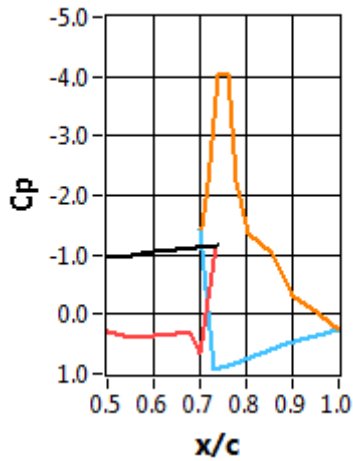
Time=41.464 s, CL=1.621



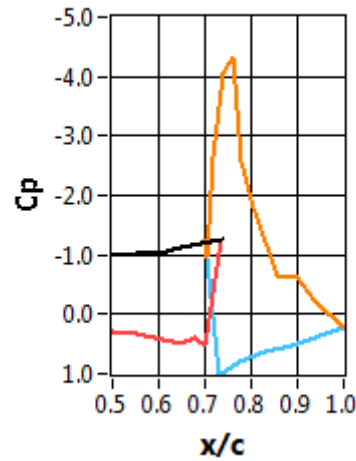
Time=41.467 s, CL=1.690



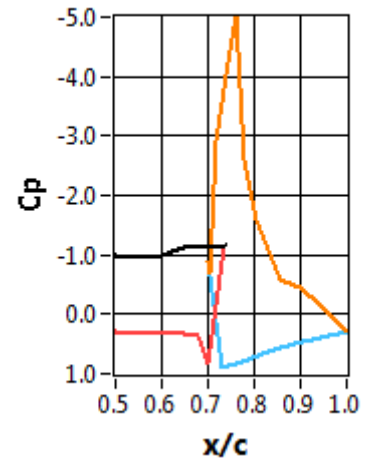
Time=41.470 s, CL=1.725



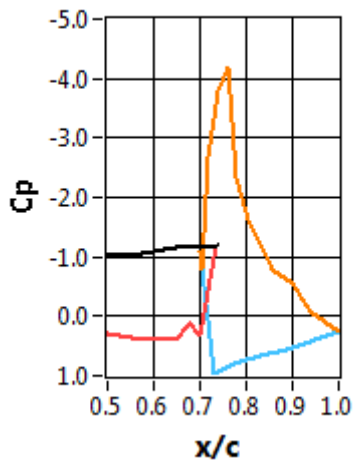
Time=41.473 s, CL=1.768



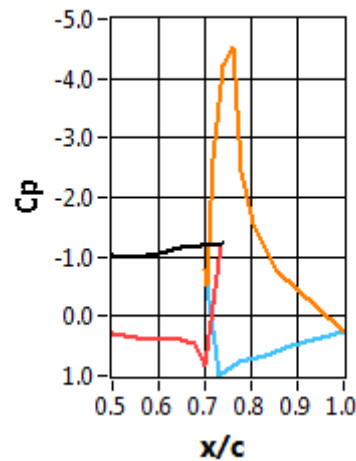
Time=41.476 s, CL=1.749



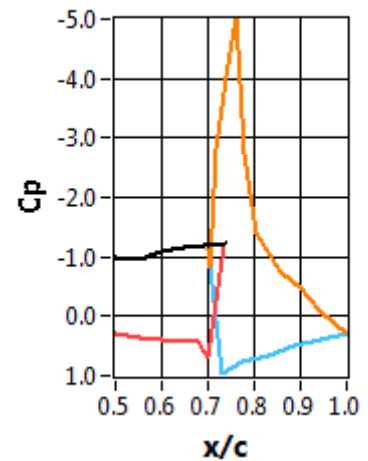
Time=41.479 s, CL=1.748



Time=41.482 s, CL=1.767



Time=41.485 s, CL=1.788



4. Environmental tests of CLC-System Prototype

4.1. Introduction to the environmental tests

This chapter is presenting an approach, test system architecture and results of the tests performed during the realization of WP4 – CLC-System Prototype Design, Production and tests.

Typical airborne equipment application and specification is described in MOPS. As a result of analysis of equipment application the range and type of environmental tests are established and specified using Environmental Qualification Form. These tests cover over twenty different areas of environmental conditions including temperature, humidity, pressure, vibration, EMC susceptibility and radiation, immunity to voltage spike and magnetic effect, fire, icing, lightning and many more.

Taking on account that the prototype of the CLC-System is connected with actuator and sensor systems which are regular off-the-shelf industrial products, the final application conditions can't be fully specified at this stage. Therefore the scope and the program of the tests is intended to check basic environmental behaviour of the CLC-System prototype.

In order to perform the environmental tests the prototype has been installed into an industrial grade enclosure and connected with sensors, actuators, power supply and communication link using specialised connectors.

Finally, the CLC-System prototype was tested according to the procedures covered in the next chapter. The tests were performed between 18th February and 11th March 2013 in environmental testing laboratory located in Institute of Aviation in Warsaw.

4.2. Scope of environmental tests of CLC-System Prototype

The CLC-System prototype was tested according to the following standard procedures:

Temperature and Altitude – section 4 of RTCA/DO-160,
Humidity – section 6 of RTCA/DO-160,
Vibration – section 8 of RTCA/DO-160

Each of the testing procedures were carried out according to the established equipment category. The following information defines equipment categories and corresponding procedure steps as well as parameters of the procedures (temperatures, pressures etc.) according to the sections of the RTCA/DO-160 standard.

Temperature and Altitude

Tests were carried out as for the Category A1 equipment, i.e. equipment intended for installation in a controlled temperature and pressurized location, on an aircraft where pressures are normally no lower than the altitude equivalent of 4600m MSL.

Humidity

Humidity test procedure were performed according to the Category A equipment requirements, i.e. standard humidity environment. This category is defined for equipment intended for installation in civil aircraft, non-civil transport aircraft and other classes, within environmentally controlled compartments of aircraft in which the severe humidity environment is not normally encountered.

Vibration

Vibration test procedure were carried out as for the Category S equipment, This category is intended to demonstrate that equipment will meet its functional performance requirements in the vibration environment experienced during normal operating conditions of aircraft.

4.3. CLC-System prototype environmental test results

Tests of the CLC-System prototype were performed according to the sections of the DO-160 specified in section 2 of this document. Detailed description of tests and conditions are presented in the table 2.

Table 2 Description of environmental test conditions

Test Description	Test Date	Test conditions	Test period
Section 4 - Temperature and Altitude	18.02.2013	-15 °C	12 ⁵⁰ - 13 ⁵⁰
	19.02.2013	+70 °C	13 ¹² - 13 ⁴²
	20.02.2013	+55 °C	7 ¹² - 10 ¹⁴
Section 6 - Humidity	21.02.2013	+40 °C, 95% rel. humidity	9 ⁴⁰ - 10 ⁴⁰
	21.02.2013	+50 °C, 95% rel. humidity	16 ⁰⁰ - 17 ⁰⁰
	22.02.2013	+38,2 °C, 95% rel. humidity.	10 ⁴⁰ - 11 ⁴⁰
Section 4 - Temperature and Altitude	26.02.2013	571,8 hPa	9 ⁰⁰ - 9 ³⁰

Section 8 - Vibration	11.03.2013	<u>Vibration</u>	
		Axis X:	
		1,25 mm; 5 ÷ 15 Hz	$7^{57} - 8^{17}$
		0,5 mm; 15 ÷ 74 Hz	$8^{18} - 8^{38}$
		100 m/s ² ; 75 ÷ 500 Hz	$8^{39} - 8^{59}$
		Axis Y:	
		1,25 mm; 5 ÷ 15 Hz	$9^{00} - 9^{20}$
		0,5 mm; 15 ÷ 74 Hz	$9^{20} - 9^{40}$
		100 m/s ² ; 75 ÷ 500 Hz	$9^{40} - 10^{10}$
		Axis Z:	
		1,25 mm; 5 ÷ 15 Hz	$10^{00} - 10^{20}$
		0,5 mm; 15 ÷ 74 Hz	$10^{20} - 10^{40}$
		100m/s ² ; 75 ÷ 500 Hz	$10^{40} - 11^{00}$

Tests were carried out according to conditions specified in particular sections of DO-160 using test temperature curves, humidity and pressure values and applying vibration stresses.

The controller was operating in all the periods specified in the applicable time slots described in the reference document sections. During the tests all required data were recorded using the data logging station.

Further analysis of the recorded data proved that controller functionality encompassing switching outputs, input signals measurements and communication data exchange operated properly during the whole test period.

5. Conclusions

.In the project ESTERA complete Closed Loop Control System (CLC-System) for fluidic active flow control (AFC) actuation at the wing's trailing edge was designed and manufactured together with the necessary controller unit. The CLC-System prototype has been tested experimentally on a two dimensional airfoil model NACA 0012 equipped with movable flap. During the tests the coefficient of the pressure measured in the point close to flap trailing edge was a parameter defining the state of the flow on the upper flap surface. This parameter was analyzed by control system which opened or closed the valves.

The tests were performed in the low speed wind tunnel T-1 (with 1.5 m diameter test section) in the Institute of Aviation, (IoA) Warsaw for Mach numbers $M = 0.1$, 0.075 and 0.05 . Wind tunnel tests were preceded by numerical calculation.

Performed wind tunnel tests of the CLC-System prototype have fully confirmed the correctness of the assumptions made for the model design as well as the correctness of its manufacturing. Tests showed the following:

- Blowing is an effective way to increase the lift coefficient achieved by the airfoil with strongly deflected slotted flap – the increase was maximally 30% of the lift coefficient without blowing. The lift increases not only due to reduction a separation zone on the flap but also due to increasing a negative pressure on the upper surface of the main airfoil.
- The tests confirmed hypothesis that the measurement of the pressure on upper-aft part of the flap (in one point only) allows on detecting the separation.
- The investigation confirmed an efficiency of the CLC-system as a way to increase lift with relatively low volume flow rate of the compressed air. Using a pulsed jets controlled by CLC-System the volume flow rate was diminished from $\dot{U} \approx 120 \text{ m}^3/\text{h}$ (steady blowing) to $\dot{U} \approx 68 \text{ m}^3/\text{h}$ (for $C_{p_c} = 0.0$) and to $\dot{U} \approx 33 \text{ m}^3/\text{h}$ (for $C_{p_c} = -0.4$).
- The increase in airfoil C_L value due to CLC-System operation was generally independent of the value of pressure coefficient used by the CLC-System as a signal for opening or closing the valves i.e. C_{p_c} .
- Duration of the one complete cycle of the CLC-System operation was about $\Delta t \approx 65 \text{ ms}$. Since the opening of the valves to the full flow attachment on the flap passes about $12 \div 14 \text{ ms}$. On the other hand since the closing of the valves to the full flow separation on the flap passes about $27 \div 28 \text{ ms}$.
- During the flap deflection (the increase of the flap deflection from $\delta = 0^\circ$ to $\delta = 40^\circ$ and decreasing from $\delta = 40^\circ$ to $\delta = 0^\circ$ was tested) the angle of attack significantly affects the beginning and end of the CLC-System operation. The increase in the airfoil angle of attack delays the start of the CLC-System operation.
- The change of the undisturbed flow velocity (in the range $M = 0.05 \div 0.1$) does not really effect on the qualitative changes in the flow around airfoil flap associated with the CLC-System operation (the changes are quantitative and only in the aerodynamic characteristic values). The decrease of the undisturbed flow velocity results in the decrease of the pressure coefficient in the nose part of the flap This decrease of the pressure coefficient is caused by a higher ratio of the air jet velocity to undisturbed flow velocity.

The environmental tests of the CLC-System prototype was performed in IoA Environmental Laboratory according to the standard procedures (temperature, altitude, humidity and vibration). The environmental tests (curried out according to RTCA/DO-160 document) and within the scope specified in Section 2 of this document show that CLC-System prototype passed the test procedures.